Coupled-cavity ring-down spectroscopy technique

Jérémie Courtois and Joseph T. Hodges*

National Institute of Standards and Technology, 100 Bureau Drive, Gaithersburg, Maryland 20899, USA
**Corresponding author: joseph.hodges@nist.gov*

Received May 14, 2012; accepted June 6, 2012;
posted June 13, 2012 (Doc. ID 168498); published August 6, 2012

We present a technique called coupled-cavity ring-down spectroscopy (CC-RDS) for controlling the finesse of an optical resonator. Applications include extending the sensitivity and dynamic range of a cavity-enhanced spectrometer as well as widening the useful spectral region of high-reflectivity mirrors. CC-RDS uses controlled feedback of the probe laser beam to a ring-down cavity, which leads to interference between the internally circulating light and that which is fed back through a cavity mirror port. Using a 74 cm long ring-down cavity and a feedback cavity with a finesse of 16, we demonstrate that this effect increases the decay time constant from 210 μs to 280 μs, corresponding to an increase of finesse from 2.7×10^5 to 3.6×10^5. Finally, we show that with the addition of a second feedback cavity, we observe ring-down times as long as ~0.5 ms, which is equivalent to $(1 - R) \approx 4.9 \times 10^{-6}$, where R is the effective mirror reflectivity.

OCIS codes: 120.6200, 140.4780, 300.1030.

Since the first measurements of optical ring-down decay signals [1], many experimental approaches have been developed that exploit the extremely long effective path lengths associated with high-finesse cavities [2]. These cavities are formed by ultrahigh-reflectivity mirrors composed of superpolished, low-scatter substrates that are coated with layers of dielectric material having variable refractive index. Of the techniques exploiting this technology, one of the most commonly implemented is cavity ring-down spectroscopy (CRDS) [3], which is based on measurement of the exponentially decaying optical power exiting the cavity. For an empty cavity with lossless mirrors (i.e., no scattering or absorption) of intensity reflectivity R and mirror-to-mirror distance L, the ring-down time constant is given by $\tau_0 = L(cT)^{-1}$ where c is the speed of light and $T = 1 - R$ is the mirror transmittance. The absorption coefficient of the cavity medium is inferred by measuring small changes in the ring-down time, and its limit of detection is nominally equal to $\varepsilon_\tau TL^{-1}$. Here ε_τ, whose magnitude is influenced by statistical effects such as signal strength and detector and digitizer noise, is the relative standard uncertainty in the measured ring-down time τ. In practice, long-term averaging of τ to improve measurement precision is often limited by uncertainty and variability in the base losses $T \times L^{-1}(c\tau_0)^{-1}$ [4,5] that are caused by interference involving unwanted reflections from external optical elements back to the ring-down cavity (RDC). This effect, known either as etaloning, spurious reflection [6], or self-mixing, increases in importance as R approaches unity. As shown below, etaloning leads to an effective RDC mirror reflectivity, R_{eff}, that can be greater or less than that of the isolated mirror. In CRDS and other cavity-enhanced experiments, etaloning is manifest by slow temporal variation and sinusoidal wavelength dependence in τ_0. This occurs because the effective base losses are sensitive to uncontrolled variations in the phase of the optical feedback (from external cavities) that are caused by drift in the relevant optical pathlengths. Since the early days of CRDS, practitioners have been familiar with etaloning effects [7], and it is now common practice to experimentally reduce this background perturbation using wedged ring-down mirrors, tilted optics, off-axis injection schemes, or antireflective coatings on every interface. Indeed, these steps are required to reach more fundamental detection limits set by the detector noise or the inherent shot noise of the light.

Nevertheless, surprisingly and to the best of our knowledge, no one has exploited the etaloning effect to intentionally alter the effective finesse of a RDC. In this letter, we show that one can substantially increase the finesse of a resonator relative to the isolated-cavity case by controlled optical feedback from an external resonator, accordingly lowering the spectrometer's detection limit. We call this technique coupled-cavity ring-down spectroscopy (CC-RDS). Furthermore, this method has the potential to improve the versatility of the spectrometer by extending the measurement dynamic range and by broadening the useful spectral bandwidth of the high-reflectivity RDC mirrors.

Figure 1 depicts the elements of a CC-RDS apparatus, which involves two coupled cavities. The principal one is a length-stabilized RDC that includes two mirrors [M_1 (flat) and M_2 (plano–concave)] with intensity reflectivities R_1 and R_2 respectively, and the other is the feedback cavity (FBC) which consists of two mirrors [M_1, feedback mirror (FBM, spherical) and a dichroic beam splitter (DBS)]. For the isolated RDC, the geometric mean value of the reflectivity is given by $R = (R_1R_2)^{1/2}$.

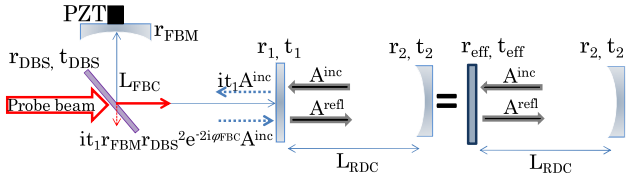

Fig. 1. (Color online) Schematic principle of the coupled-cavity ring-down spectrometer and its corresponding equivalent optical system. Once the probe-beam intensity has been interrupted, the light leaks out of the RDC at a rate dictated by its round-trip losses (isolated system). In the coupled-cavity case, the reflected field from mirror M_1, given by A^{refl}, arises from the direct reflection of the circulating field within the RDC, r_1A^{inc}, plus the portion of the circulating field in the FBC that retroreflects from the FBM and couples back into the RDC through its input mirror, $i^2t_1^2S_{\text{FBC}}$. This coupled-cavity mechanism alters the effective reflectivity of mirror M_1 in the equivalent optical system, thus altering the finesse of the RDC.

However, in the more general case of the CC-RDS system in which there is retroflection to the main RDC, R_1 and R_2 can be replaced by their respective *effective* values, which we denote by $R_{1,\mathrm{eff}}$ and $R_{2,\mathrm{eff}}$. This enables us to describe an equivalent two-mirror RDC for the coupled cavity system that takes into account the light-recycling influence of the FBC. Analysis of $R_{1,\mathrm{eff}}$ and $R_{2,\mathrm{eff}}$ requires that one include not only the principal reflection occurring at each RDC mirror but also interference by the transmitted field that is fed back through the cavity end mirror from the FBC.

We find that $R_{1,\mathrm{eff}}$ depends on the absolute amplitude reflectivity $|r_1^2|$, as in an isolated RDC system, but also depends on $t_1 = (1 - r_1^2)^{1/2}$, $\varphi_{\mathrm{FBC}} = 2\pi L_{\mathrm{FBC}}\lambda^{-1}$, r_{DBS}, r_{FBM}, t_{extra}, and C_{00}, where these terms represent the amplitude transmission of M_1 the single-pass phase shift experienced by the light within the FBC, the amplitude reflectivity of the DBS and the FBM, the net amplitude transmission through the FBC medium, and the fundamental transverse electromagnetic mode (TEM_{00}) amplitude coupling coefficient of the feedback beam (discussed below), respectively. An expression for $R_{1,\mathrm{eff}}$ is obtained by evaluating $|r_1 + r^2 t_1^2 S_{\mathrm{FBC}}|^2$, where the first term corresponds to the directly reflected part ($r_1 A^{\mathrm{inc}}$) and the second term is the feedback contribution. Here $r^2 = -1$, and $S_{\mathrm{FBC}} = C_{00} r_{\mathrm{FBM}} r_{\mathrm{DBS}}^2 t_{\mathrm{extra}}^2 e^{2i\varphi_{\mathrm{FBC}}} \sum_{n=0}^{\infty} (r_1 r_{\mathrm{FBM}} r_{\mathrm{DBS}}^2 t_{\mathrm{extra}}^2 e^{2i\varphi_{\mathrm{FBC}}})^n$ is the dimensionless circulating field amplitude, which has undergone multiple round-trips in the external FBC. Evaluating this summation leads to an effective intensity reflectivity for M_1 of

$$R_{1,\mathrm{eff}} = |r_{1,\mathrm{eff}}|^2 = \left| r_1 - C_{00} \frac{r_{\mathrm{FBM}} r_{\mathrm{DBS}}^2 t_{\mathrm{extra}}^2 t_1^2 e^{2i\varphi_{\mathrm{FBC}}}}{1 - r_1 r_{\mathrm{FBM}} r_{\mathrm{DBS}}^2 t_{\mathrm{extra}}^2 e^{2i\varphi_{\mathrm{FBC}}}} \right|^2, \tag{1}$$

where we note that (assuming $r_1 \approx 1$) the second term in the sum corresponds to the Airy transmission formula for a resonator with round-trip losses of $r_1 r_{\mathrm{FBM}} r_{\mathrm{DBS}}^2 t_{\mathrm{extra}}^2$ and phase delay of $2\varphi_{\mathrm{FBC}}$.

From Eq. 1, we can calculate the modified RDC time constant in the case of light recycling through the input mirror M_1 by the FBC as $\tau_{\mathrm{eff}} = L/(c(1 - (R_{1,\mathrm{eff}} R_2)^{1/2}))$. In Fig. 2, the blue (lower) curve shows a calculation of τ_{eff} for an ideally lossless system ($t_{\mathrm{extra}} = C_{00} = 1$) as a function of the input FBM displacement, $\Delta L_{\mathrm{FBC,Input}} = L_{\mathrm{FBC,Input}} - L_{\mathrm{FBC,Input,0}}$. These calculations are based on the CC-RDS system experimental values discussed below: $L_{\mathrm{FBC,Input,0}} = L \approx 74$ cm, $R_1 = R_2 = 99.9988\%$ (equivalent to $T = 1.2 \times 10^{-5}$ and corresponding to the measured decay time $\tau_0 = 210$ μs for the TEM_{00} mode of the isolated RDC), $R_{\mathrm{DBS}} = 0.71$ for the sagittal field polarization (s polarization) at $\lambda \approx 940$ nm and $R_{\mathrm{FBM}} = R_1$. Not surprisingly, our analysis indicates that the self-mixing effect leads to a $\lambda/2$ periodic L_{FBC}-dependent modulation in τ_{eff} about τ_0. For in-phase self-mixing of the two fields, the original value of $T_1 = 1.2 \times 10^{-5}$ for M_1 is reduced two-fold to $T_{1,\mathrm{eff}} = 5.9 \times 10^{-6}$ ($\tau_{\mathrm{eff,max}} = 280$ μs). This change in effective mirror transmittance, which is caused by the addition of the feedback resonator with a finesse of about 16 [$F = \pi\sqrt{R_m}(1 - R_m)^{-1}$, where $R_m = (R_{\mathrm{DBS}}^2 R_{\mathrm{RDC}} R_{\mathrm{FBM}})^{1/4}$ is the mean reflectivity of the FBC], corresponds to an increase in F from

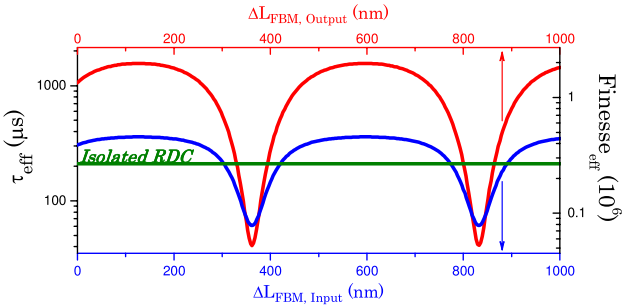

Fig. 2. (Color online) Theoretical dependence of the effective time constant τ_{eff} on changes in the input (blue/lower) and output (red/upper) FBC lengths, ΔL_{FBM}. While the latter case corresponds to an input ΔL_{FBM} that maximizes $R_{1,\mathrm{eff}}$, both cases consider lossless FBC systems. The line labeled "Isolated RDC" is the nominal observed decay time constant of the isolated system. Parameters correspond to those of our experimental configuration and are given in the text.

$\sim 2.7 \times 10^5$ (isolated ring-down cavity) to $\sim 3.6 \times 10^5$ (coupled-cavity case).

We also display in Fig. 2 (red/upper curve) the periodic behavior of τ_{eff} when one simultaneously introduces a second FBC, the "output" FBC, to recycle the light that leaks through the output mirror of the RDC (note that this FBC is not shown in Fig. 1 but is located after M_2 in a similar fashion to the "input" FBC). In these simulations, we assume $F = 31$ for the output FBC. Also we suppose that the input FBC (which reinjects the light through M_1) is fixed in length to maximize $R_{1,\mathrm{eff}}$ while the distance between M_2 and the output FBM is varied. In this case, we project that the maximum finesse equals as much as $\sim 2 \times 10^6$, with a corresponding τ_{eff} of ~1.56 ms.

We constructed an experimental system as shown in Fig. 1 to test our theoretical predictions. The system consists of a frequency-stabilized CRDS (FS-CRDS) apparatus (M_1 flat; mirror M_2 with a radius of curvature of 1 m) combined with a three-mirror linear length-stabilized FBC. The FS-CRDS cavity has a free spectral range (FSR) of ~200 MHz, and its length is stabilized to within ~1 nm by reference to a frequency-stabilized HeNe laser ($\lambda = 633$ nm) as described in [8]. To probe the RDC resonances, a single-mode (~1 MHz linewidth) continuous wave external-cavity diode laser (ECDL) at $\lambda \approx 940$ nm was launched through a single-mode fiber, mode-matched with >99% coupling efficiency, and locked to a TEM_{00} of the RDC with a low-bandwidth servo (to compensate for laser frequency drift) [8]. Ring-down signals are detected in transmission through M_2. The input FBC was formed by the DBS, a piezoelectric transducer (PZT)-actuated FBM, and M_1. The system also included an FBC locking servo that used a second frequency-stabilized HeNe laser whose optical frequency was tuned by an acousto-optic modulator (AOM). The respective cavity finesses for the RDC and input FBC at $\lambda =$ 633 nm were ~60 and ~7.5. In practice, we selected FBM positions corresponding to arbitrary points along the $\tau_{\mathrm{eff}}(\Delta L_{\mathrm{FBM}})$ curve, with an estimated precision of $\Delta L_{\mathrm{FBM}} \approx 5$ nm. To tune the FBC length, we used the AOM to vary the optical frequency of the HeNe laser to which the FBC was locked. This method gave a

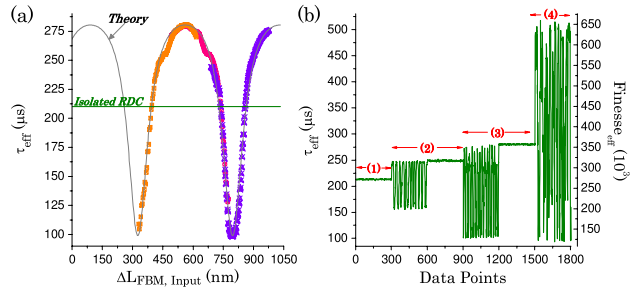

Fig. 3. (Color online) (a) Comparison of three sets of measurements with theoretical predictions given by Eq. (1). The line labeled "Isolated RDC" is the nominal observed decay time constant of the isolated system, and the curve labeled "Theory" is based on Eq. 1 with experimental parameters given in the text; (b) Measured empty cavity decay time constants together with the corresponding effective finesse. In (1) the RDC is isolated, while for cases (2) and (3) one FBC is used to change the effective finesse of the RDC through alteration of $R_{1,\mathrm{eff}}$. In the latter recycling system the finesse for the input FBC for the *s*- and *p*- polarization states of the probe beam are 7 and 18, respectively, explaining the differences in modulation depth when the FBM is dithered. Flat data regions correspond to an actively length-stabilized FBC. In (4) a second output FBC was introduced, while the input FBC length was both adjusted and maintained to maximize $R_{1,\mathrm{eff}}$.

displacement of the FBM in terms of the AOM frequency shift Δf_{AOM} as $\Delta L_{\mathrm{FBM}} = (2\Delta f_{\mathrm{AOM}}/\mathrm{FSR}) \times (\lambda_{633}/2)$ and enabled active control of the feedback cavity length over a range of ~285 nm.

In Fig. 3(a) we compare our experimental results with theoretical predictions. Three sets of measurements, with each set acquired by stepping ΔL_{FBM} and averaging 300 ring-down events per step, are displayed. Using measured parameters for all other terms appearing in Eq. 1, we found that the values $C_{00} = 0.67$ and $t_{\mathrm{extra}} = 0.95$ minimized differences between our Eq. 1 and the measured $\tau_{\mathrm{eff}}(\Delta L_{\mathrm{FBM}})$ values. The good agreement between observed and calculated values for $\tau_{\mathrm{eff}}(\Delta L_{\mathrm{FBM}})$ validates our analysis for quantitative prediction of the self-mixing effect in a two-cavity coupled system.

Note that C_{00} represents the product of two amplitude coupling terms given by $C_{00,\mathrm{FBC}} \times C_{00,\mathrm{RDC}}$, where the former represents the fraction of the light leaking out of the RDC that is coupled into the FBC, and the latter is the fraction of light leaking out of the FBC that couples back into the RDC. As deduced from Eq. 1, the highest depth of modulation in $\tau_{\mathrm{eff}}(\Delta L_{\mathrm{FBM}})$ occurs when $C_{00} = 1$. In our system, we attribute the observed 33% and 14% reduction from unity coupling efficiency in the input and output FBCs, respectively, to residual absorption (mirror, vacuum window, absorption by ambient water vapor), Fresnel losses, and unavoidable coupling into higher-order TEM_{mn} modes of either coupled cavity.

We also quantified the RDC detection limit with and without the FBC by measuring the Allan variance [9] of the ring-down time constants. In both cases, there was no evidence of deviation from single exponential decays. These measurements yielded a RDC detection limit of 6.8×10^{-11} cm^{-1} (1 s averaging time) in the latter case for $\tau_{\mathrm{eff,max}} = 280$ μs. No degradation in the averaging statistics was observed, and the detection was found to scale with the decrease in effective base losses relative to the isolated-cavity case. However, and as expected from the behavior illustrated in Fig. 2, for ΔL_{FBM} cases that yield finesse values outside of the extrema, we found that the measurement statistics were highly sensitive to small variations in ΔL_{FBM}.

The data presented in Fig. 3(b), cases 2 and 3, further illustrate our ability to manipulate the finesse of an RDC by light recycling with an input FBC. Moreover, Fig. 3(b), case 4, illustrates the effect of introducing an output FBC to simultaneously change the effective reflectivity of M_2. In this case, the cavity finesse of the output FBC is ~31 ($R_{\mathrm{DBS}} = 0.82$), and the total C_{00} amplitude fraction of the beam returning the TEM_{00} RDC mode is 86%. With both FBCs, we measured τ_{eff} up to ~0.5 ms, corresponding to an effective RDC mirror transmittance of 4.9×10^{-6}.

In conclusion, the CC-RDS light-recycling technique presented here enables one to significantly increase the finesse of an RDC or similar cavity-enhanced spectrometer. We explain this effect in terms of the change in effective reflectivity of a coupled-cavity system. In addition to lowering the spectrometer detection limit, active control of the finesse enables extension of the CRDS dynamic range and the useful spectral region of the RDC high-reflectivity mirrors. Wide dynamic range in CRDS could be exploited in high-precision laser-based measurements of isotopic ratios (e.g., for pairs of atmospheric isotopologues having disparate relative abundances) because transitions having nearly the same temperature dependencies could be probed [10]. Finally, for measurements of broadband absorption such as the water vapor continuum [11], we anticipate that slowly drifting etalons, which limit the useful averaging time and minimum detectable absorption, may be compensated by actively controlling the RDC base loss through adjustment of an FBC length.

References

1. D. Z. Anderson, J. C. Frisch, and C. S. Masser, Appl. Opt. **23**, 1238 (1984).
2. J. Ye, L.-S. Ma, and J. L. Hall, J. Opt. Soc. Am. B **15**, 6 (1998).
3. A. O'Keefe and D. A. G. Deacon, Rev. Sci. Instrum. **59**, 2544 (1988).
4. H. Huang and K. K. Lehmann, Appl. Opt. **49**, 1378 (2010).
5. A. Cygan, D. Lisak, S. Wójtewicz, J. Domysławska, J. T. Hodges, R. S. Trawiński, and R. Ciuryło, Phy. Rev. A **85**, 022508 (2012).
6. R. W. Fox and L. Hollberg, Opt. Lett. **27**, 1833 (2002).
7. D. Romanini and K. K. Lehmann, J. Chem. Phys. **99**, 6287 (1993).
8. J. T. Hodges, H. P. Layer, W. M. Miller, and G. E. Scace, Rev. Sci. Instrum. **75**, 849 (2004).
9. D. W. Allan, Proc. IEEE **54**, 221 (1966).
10. E. Kerstel and L. Gianfrani, Appl. Phys. B **92**, 439 (2008).
11. J. G. Cormier, J. T. Hodges, and J. R. Drummond, J. Chem. Phys. **122**, 114309 (2005).